



Temperature dependence of CO desorption kinetics at a novel Pt-on-Au/C PEM fuel cell anode

A. Pitois^{a,*}, A. Pilenga^a, A. Pfrang^a, G. Tsotridis^a, B.L. Abrams^b, I. Chorkendorff^b

^a Institute for Energy, Joint Research Centre, European Commission, Postbus 2, 1755 ZG Petten, The Netherlands

^b Center for Individual Nanoparticle Functionality (CINF), Department of Physics, NanoDTU, Technical University of Denmark, 2800 Kongens Lyngby, Denmark

ARTICLE INFO

Article history:

Received 7 December 2009

Received in revised form 4 May 2010

Accepted 5 May 2010

Keywords:

CO tolerance

Kinetics

Platinum

Gold

Isotope exchange

PEM fuel cell

ABSTRACT

A Pt-on-Au/C fuel cell anode catalyst has been obtained by electrochemical deposition of platinum on carbon-supported gold nanoparticles. Its composition, structure and nanoparticle size distribution have been characterised before and after the desorption experiments using microstructural techniques. The temperature dependence of the CO desorption process on this system has been investigated using isotopic exchange experiments. The CO desorption kinetics have been studied as a function of temperature and flow rate. Desorption rate constants have been measured for a temperature range between 25 and 150 °C. These desorption rate constants have been compared with the benchmarking desorption rate data obtained for the commercial Pt/C catalyst under similar experimental conditions. A comparable desorption rate constant for the Pt-on-Au/C and Pt/C systems has been obtained at 25 °C. The dependence in temperature of the desorption rate constants for the novel Pt-on-Au/C system is however much lower than that observed for the Pt/C system. This suggests that the nature of the substrate has a significant influence on the catalyst surface properties. It shows that, in surface-modified catalysts, the interactions between underlayer and overlayer materials are worthy of consideration, since they can significantly modify the intrinsic properties of the active sites. The kinetics of the CO desorption process have been discussed with regard to the CO tolerance issue at the PEM fuel cell anode.

© 2010 Elsevier B.V. All rights reserved.

1. Introduction

Among the different types of fuel cells, proton exchange membrane fuel cells (PEMFCs) are being developed for transportation, portable and small stationary applications [1]. Platinum is currently a catalyst component or catalyst of choice for the anode and cathode processes, respectively due to the high current densities obtained [2]. The platinum catalyst is however subject to poisoning by CO for PEMFC systems operating with reformat gas [3]. Platinum–ruthenium catalysts have attracted considerable interest in recent years as highly active and more CO tolerant anode catalysts [4,5]. A mechanistic understanding at the atomic level of the fundamental physicochemical processes involved in improving CO tolerance is however still required if we are to develop a novel low cost and CO tolerant competitor to the current state-of-the-art Pt and PtRu anode catalysts. Three mechanisms have been suggested to explain improved CO tolerance of PtRu catalyst compared to pure Pt: the bifunctional mechanism [6–12], the ligand effect mechanism [11–15] and the “detoxification” mechanism [16–18]. Electronic ligand and strain effects were also proposed

in CO and CO/H₂ temperature-programmed desorption studies on bimetallic Pt/Ru(0001) surfaces [19]. Whereas the bifunctional and ligand effect mechanisms explain the improved CO tolerance by a favoured electrochemical oxidation of CO at the PtRu surface, the “detoxification” mechanism proposes a lower equilibrium CO surface coverage at the PtRu surface, simply via the CO adsorption/desorption process. Therefore, both the electrochemical CO oxidation and the equilibrium attained through the adsorption/desorption process should be considered as physicochemical processes affecting the CO tolerance, since the kinetically predominant of these two processes will govern the CO surface coverage at steady-state.

In the search for a cheaper and more CO tolerant, yet highly active, competitor to the current state-of-the-art Pt and PtRu catalysts for the hydrogen oxidation reaction, core–shell and alloy nanoparticle catalysts have been considered as promising candidates, since the physicochemical properties of core–shell and alloy systems can potentially be superior compared to their individual components. A combined Pt–M (where M is another metal) core–shell or alloy system could potentially minimise the amount of expensive Pt (while maintaining high activity) and increase the CO tolerance by stabilising Pt against CO poisoning [20–22]. Recently, density functional theory calculations have identified the Pt–Au-based systems as potential candidates for the hydrogen evo-

* Corresponding author. Tel.: +31 224 565308; fax: +31 224 565625.
E-mail address: aurelien.pitois@ec.europa.eu (A. Pitois).

lution reaction [23,24]. A high catalytic activity of the Pt–Au-based systems, even higher than that of pure Pt, has been reported for some specific catalytic reactions such as hexane conversion [25], ethylene glycol oxidation [26], methanol oxidation [27–32] and formic acid oxidation [32–35]. The increase in catalytic activity of the Pt-modified Au nanoparticles has been explained by the utilisation enhancement of Pt in these electrocatalysts and a possible enhancement effect of Au atoms [27,22,35]. The structure of the Pt–Au-based system, core–shell or alloy, as well as the relative ratios of each component have been demonstrated to affect, in most cases, the performance of the system. Thus, the deposition of Pt particles of various sizes on Au substrate has been shown to affect the level of CO oxidation [36,37]. This has been explained by the variation in Pt particle size and possibly also Pt nanoparticles–Au substrate interactions. A clear interaction between Au and Pt and its effect on catalytic reactivity has been demonstrated, since a stronger CO binding has been observed when Pt was deposited as an overlayer on a Au(111) substrate [38]. This increase in reactivity for CO on Pt has been attributed to the correlation between adsorbate binding energy changes with a shift in the position of the Pt overlayer d-band centre. Extensive studies have been also performed on the interactions of CO with other bimetallic surfaces such as PdAu [39–42].

The aim of the present work is to investigate for a novel potential PEM fuel cell anode catalyst the CO desorption process over a temperature range that is of relevance to the operating PEM fuel cell. The fundamental understanding of the CO desorption process involved in improving CO tolerance is expected to help developing novel low cost and CO tolerant PEM fuel cell anode catalysts. A temperature range between 25 and 150 °C has been used for the measurements, since the research community is currently engaged in the development of new PEMFC membranes capable of operating at higher temperatures than the current industry standard, the Nafion membrane, limited by its need for humidification by water to less than 100 °C. The kinetics of CO desorption from the benchmarking commercial Pt/C and PtRu/C catalysts have been investigated at room temperature and as a function of the temperature under dry conditions and in the absence of a potential [17–19,43,44]. The measured rates of desorption are high compared with the rates of oxidation measured from polarisation curves obtained with high concentrations of CO in argon. Recently, the CO exchange rates were measured at room temperature, under dry conditions and, for the first time, in the presence of a potential, on a Pt electrode for CO concentrations ranging from 1% CO in argon to 100% CO [45]. A fast exchange of adsorbed CO compared to the extremely low adsorbed CO oxidation rate was reported at potentials far below the onset of oxidation. Comparing the results for CO isotope exchange experiments under the electrochemical environment with the results from the gas phase isotope exchange experiments on supported Pt catalyst [20], it was found that the presence of electrolyte and the applied potential do not cause a significant stabilisation of the adlayer against exchange. Therefore, it was suggested that, at a typical PEMFC operation temperature of 80 °C, CO_{adsorbed} desorption will be sufficiently fast in an electrochemical environment that it can contribute significantly to keep the steady-state CO_{adsorbed} coverage at tolerable levels even in contact with CO-contaminated feed gas, if the CO concentration is not too high.

All these investigations suggest that the adsorption/desorption process may have a significant influence with regard to the CO poisoning effect at PEMFC anodes. No exchange rate on PEMFC anode catalysts other than the benchmarking commercial Pt/C and PtRu/C catalysts has however been investigated. There is nevertheless a need to determine the CO desorption rate constants on novel PEMFC anode catalysts for a better understanding of the CO tolerance issue and if we are to develop novel low cost and CO tolerant

catalysts based on the fundamental understanding of the processes involved.

In this study, a Pt-on-Au/C fuel cell anode catalyst has been obtained by electrochemical deposition of platinum on carbon-supported gold nanoparticles. Its composition, structure and nanoparticle size distribution have been characterised, before and after the desorption experiments, using microstructural techniques such as X-ray diffraction, scanning electron microscopy, transmission electron microscopy and X-ray photoelectron spectroscopy. The CO desorption kinetics have been investigated as a function of temperature and flow rate. Desorption rate constants have been deduced from the CO desorption kinetics data and have been compared with the benchmarking desorption rate data obtained for the commercial Pt/C and PtRu/C catalysts under similar experimental conditions.

2. Materials and methods

2.1. Material synthesis

Pt-on-Au catalyst nanoparticles supported on Vulcan carbon XC72 and bound to Toray carbon paper gas diffusion layers with a Teflon binder were used for the CO desorption kinetic experiments. A Teflon binder was used instead of a Nafion binder to ensure the ability to perform the experiments up to a temperature of 150 °C, the Nafion binder being limited to temperatures below 100 °C for water management reasons. The Au nanoparticles supported on Vulcan carbon XC72 powder were purchased with a loading of 20% from E-TEK. The Au nanoparticles were mixed into a 2.5:1 ethanol (96%):Teflon slurry and drop-cast onto Toray carbon paper gas diffusion layers. Pt was deposited onto the Au/C-paper system electrochemically from a Pt mesh counter electrode (99.99%) using anodic dissolution of Pt and Pt ion transfer from the Pt mesh counter electrode to the surface of the Au working electrode. Using the Au sample as the working electrode, a Pt mesh as the counter electrode, and a saturated calomel electrode as the reference electrode, the potential of the working electrode was swept at 50 mV/s during cyclic voltammetry to potentials greater than the corrosion potential for Pt (~+1.18 V vs. NHE) [46]. The potential applied to the working electrode was between –0.35 and +1.0 V vs. SCE, which, using an electrolyte with a pH ~ 0.3–0.4, ranged from ~–0.1 to +1.27 V vs. NHE. During deposition of the Pt from the counter electrode, the hydrogen evolution reaction was monitored for an increase in activity. The cycling for Pt deposition was performed during a 24 h period, leading to a maximum current, which coincides with a minimisation of the Au reduction peak. At this point, a grey discoloration of the Au surface was visible to the eye and Pt HUPD (hydrogen under potential deposition) features were apparent. Based on the Pt HUPD features, the Pt amount deposited on the Au/C nanoparticles can be estimated to a few monolayers. The electrochemical characterisation of the Pt-on-Au system using cyclic voltammetry was given in [47].

All gases used (argon, hydrogen, 1000 ppm ¹²CO in argon mixture and 1% ¹³CO in argon mixture) were obtained from Linde and were of the highest commercially available purity. For the 1% ¹³CO in argon gas mixture, the CO was enriched to the ratio 99% ¹³CO/1% ¹²CO.

2.2. Methods

2.2.1. Microstructural characterisation of the Pt-on-Au/C system Scanning electron microscopy

The morphology of the Pt-on-Au/C surface, both before and after the desorption experiments up to 150 °C, was investigated using a Zeiss Supra 50 field-emission gun scanning electron microscope.

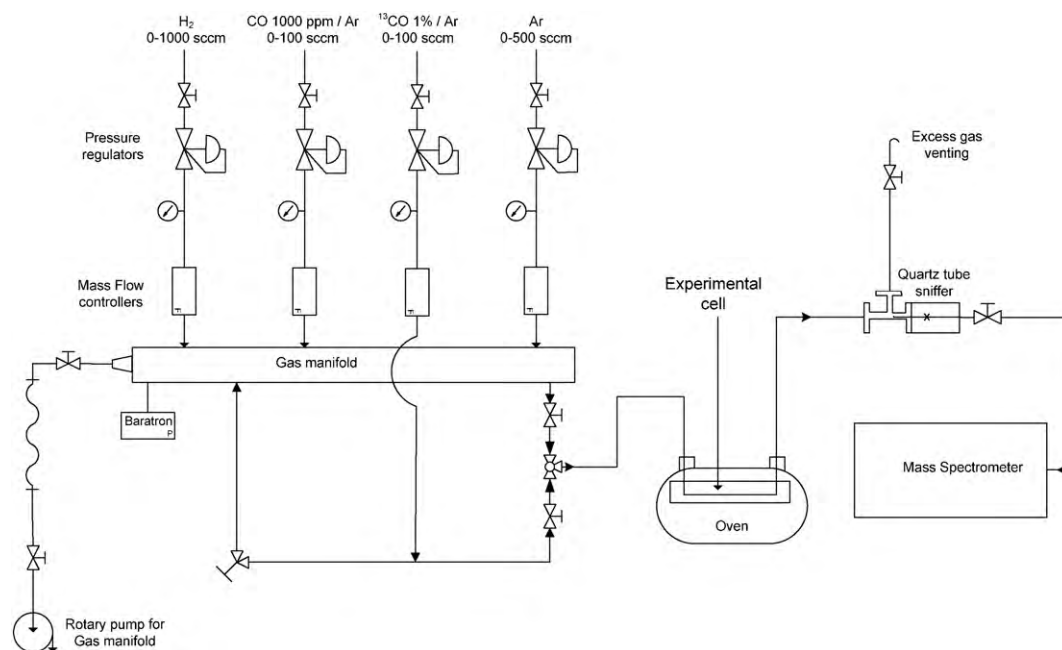


Fig. 1. Experimental setup used for the kinetic study of CO desorption.

Transmission electron microscopy

Materials scraped from the catalyst layer of tested and untested samples were characterised using a FEI Tecnai 20 transmission electron microscope operated at 200 kV with a LaB₆ filament. The catalyst dispersion and particle size distribution were assessed by the observation of a large representative number of catalyst nanoparticles (more than 200 nanoparticles).

X-ray diffraction

Characterisation of the bulk composition of the synthesised Pt-on-Au catalyst nanoparticles was performed using a Philips PW 3830 X-ray diffraction apparatus, both before and after the desorption experiments up to 150 °C.

X-ray photoelectron spectroscopy

Characterisation of the surface composition of the synthesised Pt-on-Au catalyst nanoparticles was performed using a X-ray photoelectron spectroscopy apparatus (Physical Electronics Industries) with a non-monochromatic Al K α source. The scans were recorded with a pass energy of 50 eV, a step size of 0.2 eV, and 250 ms/step. Glancing angle measurements were performed to access the nearer surface region.

2.2.2. CO desorption kinetics from the Pt-on-Au/C system

CO desorption kinetic experiments were performed in a flow cell using circular catalyst samples of diameter 3.6 cm. A gas dosing system allowed a fast interchange between various gases. The intrinsic delay of the system when switching gases was demonstrated negligible on the experiments for the conditions used and there was no significant increase in the cell pressure due to the resistance cell/sample, when varying the flow rate [17]. The gas outlet was extracted from the flow cell via a quartz tube sniffer and both its composition and content were measured in “real time” using a quadrupole mass spectrometer. An oven was used to set the temperature of the cell. The uncertainty on the temperature was ± 2 °C. The experimental setup is given in Fig. 1. The procedure for the determination of the CO desorption kinetics was described in detail in [17,18]. In summary, the catalyst surface was initially saturated by isotopically labelled ¹³CO at a given temperature using a 1% ¹³CO in argon gas mixture in order to completely cover the catalyst surface with ¹³CO. The residual ¹³CO was then removed from

the flow cell using argon. In order to obtain the desorption profile for ¹³CO, natural ¹²CO at a concentration of 1000 ppm in argon was allowed to flow through the cell and the mass 29 corresponding to ¹³CO was measured by a mass spectrometer. This procedure, close to a steady-state isotopic transient kinetic analysis (SSITKA) procedure, was already used successfully for similar studies [17,18] and has the advantage to reduce the required time for each data point. This procedure was performed at various flow rates (60, 90 and 120 ml/min) for a fixed CO concentration of 1000 ppm and a wide range of temperatures (25, 50, 75, 100, 125 and 150 °C).

3. Results and discussion

3.1. Microstructural characterisation of the Pt-on-Au/C system

3.1.1. Morphology of the Pt-on-Au/C surface

The morphology of the Pt-on-Au/C surface has been investigated using scanning electron microscopy and a characteristic scanning electron micrograph is shown in Fig. 2. No significant differences

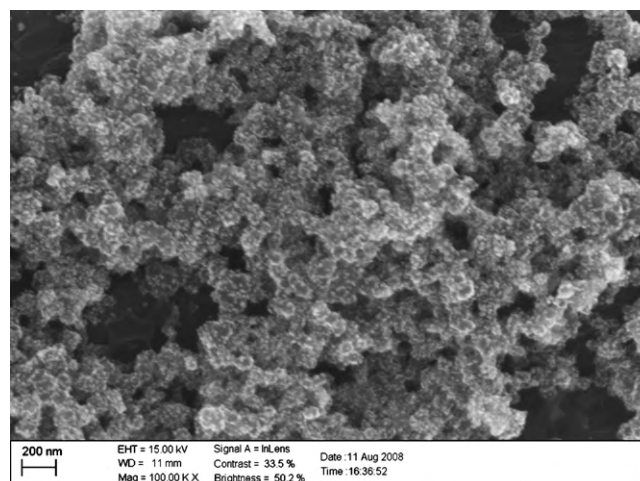


Fig. 2. Scanning electron micrograph of the Pt-on-Au/C surface.

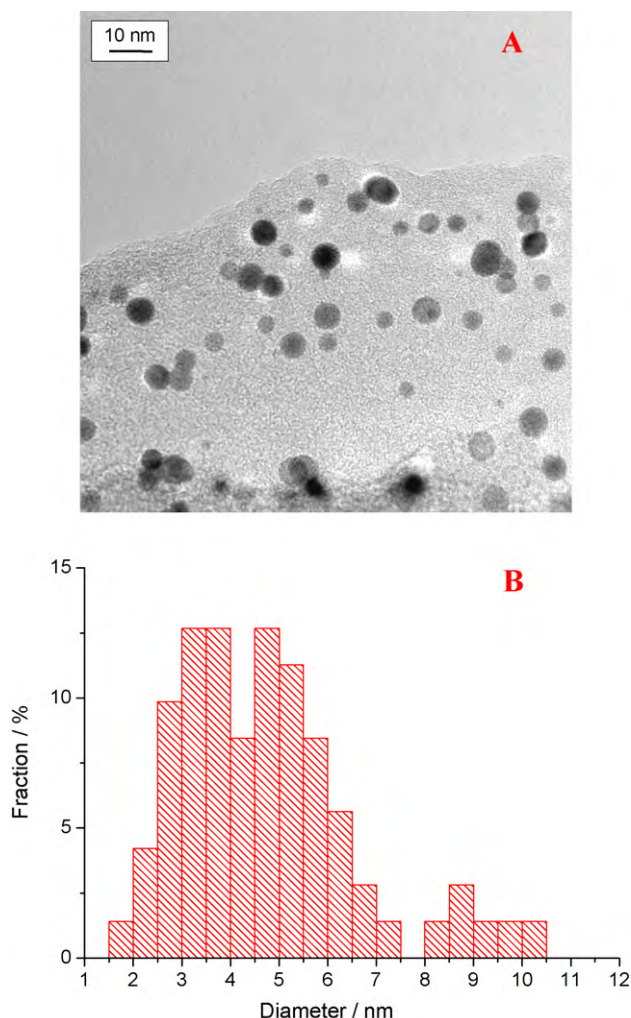


Fig. 3. (A) Transmission electron micrograph of single Pt-on-Au catalyst nanoparticles and (B) size distribution of the Pt-on-Au catalyst nanoparticles.

of the catalyst morphology before and after the desorption experiments up to 150 °C were observed.

3.1.2. Dispersion and size distribution of the Pt-on-Au catalyst nanoparticles

The dispersion and size distribution of the Pt-on-Au catalyst nanoparticles have been studied by transmission electron microscopy. A transmission electron micrograph of single Pt-on-Au catalyst nanoparticles is shown in Fig. 3A. The Pt-on-Au catalyst nanoparticles appear finely dispersed on the carbon support and thus present a high surface area. The size distribution of the catalyst nanoparticles has been assessed by transmission electron microscopy using a large representative number of catalyst nanoparticles (more than 200 single nanoparticles) and is shown in Fig. 3B. The average catalyst nanoparticle size is 4.1 ± 0.8 nm and sizes range from 2 to 10 nm, showing a quite high heterogeneity in particle size for the investigated sample. An average catalyst nanoparticle size of 4.7 ± 0.8 nm and a similar size range have been found after the desorption experiments up to 150 °C, indicating on average no significant change in the catalyst particle size due to thermal treatment.

3.1.3. Composition of the Pt-on-Au catalyst nanoparticles

X-ray diffraction (XRD) and X-ray photoelectron spectroscopy (XPS) have been used to characterise the composition of the

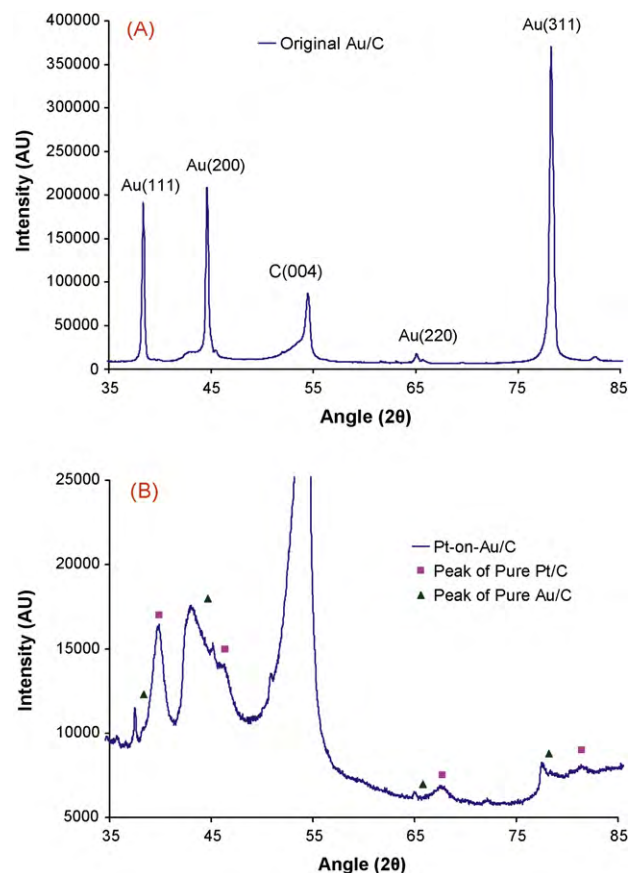


Fig. 4. (A) X-ray diffraction pattern of the Au/C catalyst nanoparticles before electrochemical deposition of Pt and (B) X-ray diffraction pattern of the Pt-on-Au/C catalyst nanoparticles (after electrochemical deposition of Pt on the Au/C catalyst nanoparticles).

Pt-on-Au catalyst nanoparticles. These two techniques are complementary, since XRD provides information on the average composition of the catalyst nanoparticle whereas XPS is a surface-specific technique. The XRD patterns of the original Au/C system and of the synthesised Pt-on-Au/C system are presented in Fig. 4A and B respectively. Similar acquisition times of XRD measurements have been used for the characterisation of these two systems. The XRD pattern presented in Fig. 4A is representative of carbon-supported gold nanoparticles. The peak located at a 2θ value of about 54° in the XRD pattern is referred to the carbon support and shows the same intensity for the two systems. The other peaks are characteristic of face-centred cubic (fcc) crystalline Au, corresponding to the planes (1 1 1), (2 0 0), (2 2 0) and (3 1 1). On the XRD pattern representative of the synthesised Pt-on-Au/C system, it can be observed that Au peaks are shifted to lower 2θ values, when compared to the Au/C XRD pattern presented in Fig. 4A and to the 2θ values of pure Au given by the Joint Committee on Powder Diffraction Data. This suggests the formation of an alloy involving the incorporation of Pt atoms into the fcc structure of Au. The overlap of the Au and carbon diffraction peaks may also be a reason for the negative shift of the Au(2 0 0) peak. The low intensity of the shifted Au peaks, when compared to the intensity of the peaks obtained in Fig. 4A for the pure crystalline Au nanoparticles, may indicate a low crystallinity for this phase, expected for an alloy. Unshifted Pt peaks are also observed on the XRD pattern of the Pt-on-Au/C system. This suggests the presence of a crystalline Pt phase in this system. Thus these results suggest that the Pt-on-Au catalyst nanoparticles may be constituted of an alloy phase rich in Au, in which Pt atoms have been incorporated, and of a pure crystalline Pt phase.

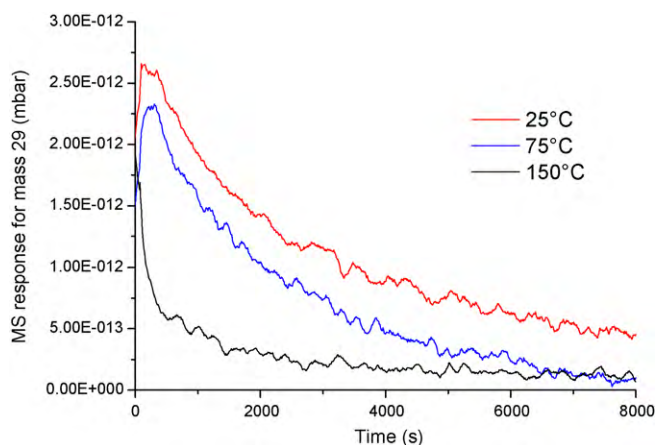


Fig. 5. Mass spectrometer traces for mass 29 (^{13}CO) on switching to 1000 ppm ^{12}CO in argon for various temperatures (25, 75 and 150 °C) at a fixed flow rate of 120 ml/min.

The characterisation of the surface composition of the synthesised Pt-on-Au catalyst nanoparticles, investigated by X-ray photoelectron spectroscopy, has been already reported in detail in [47]. Results suggest that the surface is completely covered with Pt, in good agreement with the cyclic voltammetry results and the visual observation of a grey coloration of the nanoparticle surface during the electrochemical deposition of Pt. Therefore, the synthesised Pt-on-Au catalyst nanoparticles may be constituted of a core alloy phase rich in Au, in which Pt atoms have been incorporated, and of a thin Pt film at the surface.

3.2. CO desorption kinetics from the Pt-on-Au/C system

The desorption kinetics of adsorbed isotopically labelled ^{13}CO in the presence of natural ^{12}CO at a 1000 ppm concentration in the gas phase were studied as a function of temperature (25–150 °C) and flow rate (60–120 ml/min). The relationships between the ^{13}CO desorption profile and the kinetics of the CO desorption process are explained in detail elsewhere [17].

3.2.1. Temperature dependence

Mass spectrometer traces for mass 29 (^{13}CO) on switching to 1000 ppm ^{12}CO in argon are shown in Fig. 5 for various temperatures (25, 75 and 150 °C) at a fixed flow rate of 120 ml/min. The ^{13}CO desorption kinetics increase with increasing temperature and the area under the exchange curve decreases with increasing temperature across the temperature range investigated. This behaviour is similar to that observed previously for both Pt/C and PtRu/C catalysts for a ^{12}CO concentration of 1000 ppm under similar experimental conditions [17,18], and to that observed for the PtRu/C catalyst for ^{12}CO concentrations varying from 100 to 500 ppm [43].

Assuming that at infinite time, all ^{13}CO molecules will be exchanged with ^{12}CO molecules, the relative coverage of CO exchanging can be deduced from the area under the ^{13}CO desorption curves. The relative coverage values vs. temperature for the data obtained at a fixed flow rate of 120 ml/min are given in Fig. 6. All data have been normalised against a value of 1 for the data obtained at 25 °C, thus giving a relative, rather than an absolute coverage. The relative CO coverage decreases with increasing temperature. This trend is similar to that observed in previous studies for both Pt/C and PtRu/C catalysts under similar experimental conditions [17,18,43]. The relative coverage decreases strongly for temperatures higher than 50 °C. The linear decrease for the relative CO coverage per degree Celsius between 50 and 150 °C is $6.9 \times 10^{-3} \text{ } ^\circ\text{C}^{-1}$. This decrease rate is higher than that observed

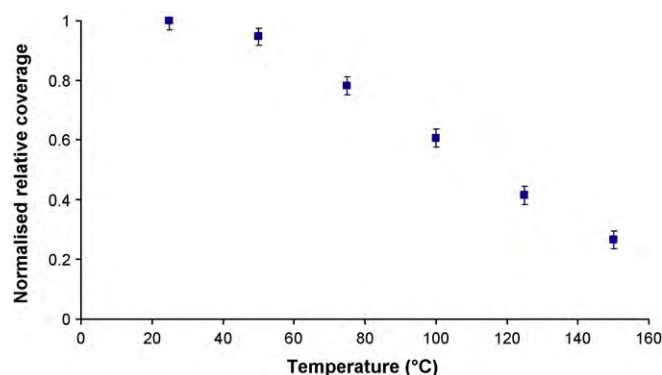


Fig. 6. Normalised relative CO coverage values vs. temperature (^{13}CO peak area for exchange at 1000 ppm CO in Ar at a flow rate of 120 ml/min).

previously for both Pt/C and PtRu/C catalysts under similar experimental conditions, i.e. $2.3 \times 10^{-3} \text{ } ^\circ\text{C}^{-1}$ for Pt/C between 50 and 150 °C, and $4.0 \times 10^{-3} \text{ } ^\circ\text{C}^{-1}$ for PtRu/C between 75 and 150 °C respectively. This indicates a stronger decrease in relative coverage with increasing temperature for the Pt-on-Au/C system, as compared to the Pt/C and PtRu/C systems. It has, however, to be pointed out that the initial absolute coverages (per surface atom) are probably very different for these various surfaces and thus that these observations refer only to the relative change in CO surface coverage as a function of temperature.

3.2.2. Flow rate dependence

The flow rate dependence of the CO exchange is shown in Fig. 7 at a fixed temperature of 50 °C and for flow rates ranging from 60 to 120 ml/min. There is a slight flow rate dependence of the CO exchange. This dependence on flow rate was already observed extensively in previous similar studies during the desorption measurements. A strong flow rate dependence was observed for both Pt/C and PtRu/C at 1000 ppm CO in argon, for temperatures higher than room temperature and for flow rates higher than 30 ml/min [17,18], as well as for the PtRu/C catalyst at CO concentrations higher than 100 ppm, for temperatures higher than room temperature and for flow rates higher than 90 ml/min [43]. This flow rate dependence was attributed to a significant readsorption of ^{13}CO during the desorption experiments and consequently the gradients of the plot shown in Fig. 7 correspond only to an apparent rate of desorption, which is dependent on the flow rate and lower than the actual rate. It has however to be pointed out that the flow rate dependence observed for the Pt-on-Au/C catalyst is not as strong

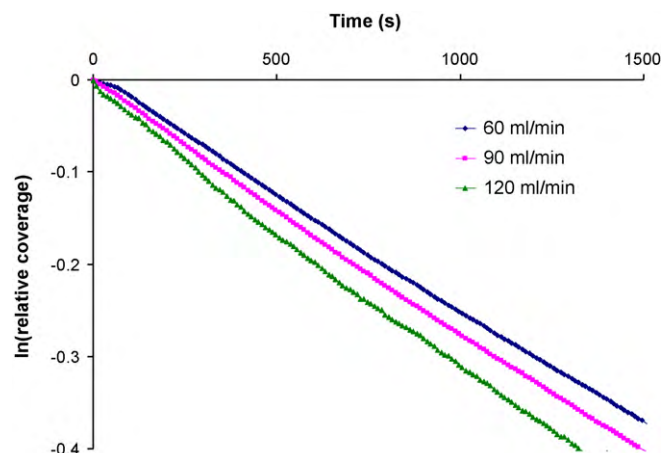


Fig. 7. Flow-rate dependence of the CO exchange at 50 °C.

as that observed for the Pt/C and PtRu/C catalysts, and thus that the degree of ^{13}CO readsorption during the desorption experiments is lower for this novel catalyst as compared to the Pt/C and PtRu/C catalysts.

3.2.3. Determination of the desorption rate constants

Using a method similar to Xu et al. [48] and assuming pseudo-steady-state conditions, the decay curve for the ^{13}CO concentration, C , can be given, in case of flow rate dependence, by the equation:

$$C = \frac{\theta_{\text{CO}} k^-}{q + \theta_{\text{CO}} k^- / C_0} \exp \left[-\frac{k^-}{1 + \theta_{\text{CO}} k^- / q C_0} t \right] \quad (1)$$

where C is the ^{13}CO concentration at time t , C_0 is the initial ^{13}CO concentration, q is the flow rate, θ_{CO} is the coverage and k^- is the desorption rate constant.

Therefore, the slope of the $\ln(\text{relative CO coverage})$ vs. time plot can be defined as an apparent rate of desorption k_{apparent} (dependent on the flow rate):

$$k_{\text{apparent}} = \frac{k^-}{1 + \theta_{\text{CO}} k^- / q C_0} \quad (2)$$

Rearranging gives the following equation, which enables the determination of the desorption rate constant k^- :

$$\frac{1}{k_{\text{apparent}}} = \frac{1}{k^-} + \frac{\theta_{\text{CO}}}{C_0} \frac{1}{q} \quad (3)$$

And so a plot of $1/k_{\text{apparent}}$ vs. $1/q$ should provide a linear response, with an intercept of $1/k^-$, k^- being the desorption rate constant. Similar plots using a wide range of flow rates were already used for the determination of the desorption rate constants on both Pt/C and PtRu/C at a fixed 1000 ppm CO concentration [17,18] and a very good linearity was found. The plot used in this study for the determination of the desorption rate constants for the novel Pt-on-Au/C system at a fixed 1000 ppm CO concentration is given in Fig. 8 for the wide range of investigated temperatures. The desorption rate constants k^- for the Pt-on-Au/C system are given as a function of the temperature (25, 50, 75, 100, 125 and 150 °C) in Table 1. The desorption rate constants increase with increasing temperature. This expected behaviour is similar to that already observed for both Pt/C and PtRu/C under similar experimental conditions [17,18]. The dependence in temperature of the desorption rate constants for this novel Pt-on-Au/C system is however much lower than that observed for both Pt/C and PtRu/C. Whereas the desorption rate constants are comparable for the Pt-on-Au/C and Pt/C systems at 25 °C ($2.4 \times 10^{-4} \text{ s}^{-1}$ vs. $4.0 \times 10^{-4} \text{ s}^{-1}$), this is no more true for temperatures higher than 25 °C. When the temperature is increased

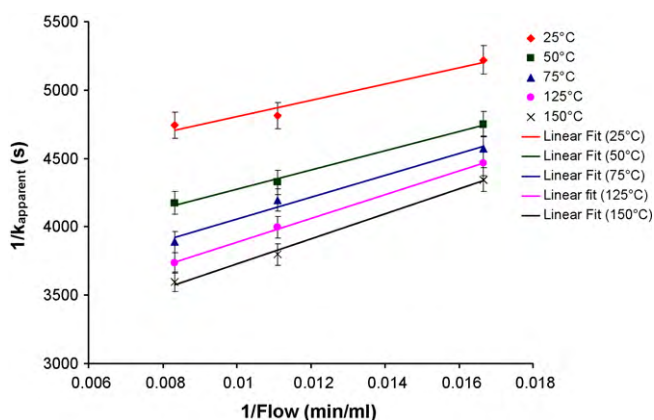


Fig. 8. Determination of the desorption rate constants at various temperatures and for a fixed CO concentration of 1000 ppm, by plotting $1/k_{\text{apparent}}$ vs. the inverse flow rate.

Table 1

Desorption rate constants k^- and equivalent CO oxidation current densities j obtained for a CO concentration of 1000 ppm at various temperatures (25–150 °C). The uncertainty on the values is 4%.

Temperature (°C)	k^- (s^{-1})	j ($\mu\text{A cm}^{-2}$)
25	2.4×10^{-4}	1.15
50	2.8×10^{-4}	1.34
75	3.1×10^{-4}	1.49
100	3.3×10^{-4}	1.58
125	3.4×10^{-4}	1.63
150	3.6×10^{-4}	1.73

from 25 to 150 °C, the desorption rate constants increase slightly from 2.4×10^{-4} to $3.6 \times 10^{-4} \text{ s}^{-1}$ for this novel Pt-on-Au/C system, whereas the desorption rate constants increase from $4.0 \times 10^{-4} \text{ s}^{-1}$ to more than $3 \times 10^{-1} \text{ s}^{-1}$ for the benchmarking Pt/C system. This suggests a significant influence of the nature of the substrate on the catalyst surface properties. Strong Pt–Au substrate interactions were already reported by CO stripping analysis for Pt-modified Au nanoparticles [30]. A positive shift in peak potentials of CO stripping with increasing Pt coverage on Au substrate was observed and was attributed to a stronger Pt–CO bonding or a weaker ensemble effect. This strong Pt–CO bonding on Au substrate was predicted by Hammer–Norskov d-band centre model [49]. In the d-band centre model, the Pt d-band centre can be up shifted on Au, and this can be related to a strengthened Pt–CO bonding. This strengthened Pt–CO bonding may explain the different behaviour of the Pt-on-Au/C and Pt/C systems for their temperature-dependent CO desorption kinetics. It shows that, in surface-modified catalysts, the interactions between underlayer and overlayer materials are worthy of consideration, since they can significantly modify the intrinsic properties of active sites. Such a promotional effect of the Au core was already reported for the CO electrooxidation reaction and was found dependent on the Pt film thickness [50–52]. It can also be noted that the measured desorption rates for the Pt-on-Au/C system are much lower than those measured as a function of the temperature for the commercial PtRu/C catalyst (from $3.2 \times 10^{-3} \text{ s}^{-1}$ at 25 °C to $2.0 \times 10^{-1} \text{ s}^{-1}$ at 150 °C).

With regard to the issue of CO tolerance, the kinetics of the CO desorption and CO electrooxidation processes cannot be directly compared for the investigated system due to unavailability of CO oxidation rate values. The measured desorption rate constants can however be converted to equivalent CO oxidation current densities for future comparison of the kinetics of the CO desorption and electrochemical CO oxidation processes. To perform this conversion, it has been assumed that the number of Pt sites is $1.50 \times 10^{15} \text{ cm}^{-2}$ (close-packed Pt(1 1 1)) and that two electrons are oxidised per CO molecule. The calculated equivalent CO oxidation current densities are given in Table 1. The equivalent CO oxidation current densities calculated for this novel Pt-on-Au/C system range from $1.15 \mu\text{A cm}^{-2}$ at 25 °C to $1.73 \mu\text{A cm}^{-2}$ at 150 °C. They can be compared, to a certain extent, with the rates of CO oxidation measured from polarisation curves on Pt for 2% CO in argon and for a temperature of 62 °C. They appear to be large, since they would require a significant overpotential of approximately 0.4V, which is not observed as a potential loss for fuel cells operating at this temperature [7]. This suggests that, in the fuel cell environment, the CO desorption process is likely to play a significant role in the CO tolerance issue: the CO desorption process may be kinetically predominant compared to the electrochemical CO oxidation process and the “detoxification” mechanism may be the major mechanism to explain the CO tolerance for this novel Pt-on-Au/C system. It has however to be pointed out that these conclusions are “first approach” conclusions due to the unavailability of CO oxidation data for the investigated system, and thus that CO oxidation data for this Pt-on-Au/C system need to be measured, if we are to val-

idate these “first approach” conclusions. It can be remarked that recent density functional theory calculations provide support to these “first approach” conclusions, since Koper et al. [12] found that, within fuel cell operating conditions, a decrease in steady-state CO coverage, which would be a driving force for the CO exchange, may be expected due to an electronic effect. It has however to be stressed that the desorption rate constants determined in this study have been measured in the absence of humidification or a potential field and therefore in a simplified adsorption environment. The presence of humidification and potential could play an important role in the balance between desorption and CO oxidation via the bifunctional mechanism within the operating fuel cell environment. Density functional theory calculations have in particular predicted that raising the potential leads to an increase in the rate of hydrogen absorption, water dissociation, CO oxidation and hydrogen oxidation because of the strong potential-dependence of the reactions [53]. Future studies will attempt to take into account humidification and potential field for a more accurate determination of the CO desorption rate constants in a real fuel cell environment. Knowledge on the dissociative H₂ adsorption behaviour in the presence of CO impurities has also to be obtained, since the balance between the kinetics of CO adsorption and H₂ adsorption is an important factor for the CO tolerance issue. This temperature-dependent kinetics study of the CO desorption process on a novel Pt-on-Au/C PEMFC anode catalyst supplements the literature data obtained previously for the more traditional Pt and PtRu catalysts [17,18,43]. The determination of the CO desorption rate constants on novel PEMFC anode catalysts is believed to be of added value for a better understanding of the CO tolerance issue at PEMFC anodes and if we are to develop novel low cost and CO tolerant catalysts based on the fundamental understanding of the processes involved.

4. Conclusions

A novel carbon-supported Pt-on-Au fuel cell anode catalyst, obtained by electrochemical deposition of Pt on Au/C nanoparticles, has been characterised by a number of microstructural techniques, i.e. X-ray diffraction, scanning electron microscopy, transmission electron microscopy and X-ray photoelectron spectroscopy. Results suggest that the synthesised Pt-on-Au catalyst nanoparticles are constituted of a core alloy phase rich in Au, in which Pt atoms have been incorporated, and of a thin Pt film at the surface. The temperature dependence of the CO desorption process on this novel fuel cell anode catalyst has been determined from CO isotope exchange experiments for a 1000 ppm CO in Ar concentration. Desorption rate constants, ranging from $2.4 \times 10^{-4} \text{ s}^{-1}$ at 25 °C to $3.6 \times 10^{-4} \text{ s}^{-1}$ at 150 °C, have been obtained for this range of temperature. At 25 °C, the desorption rate constants obtained for the Pt-on-Au/C and Pt/C systems are comparable. The dependence in temperature of the desorption rate constants for the novel Pt-on-Au/C system is however much lower than that observed for the Pt/C system. This suggests that the nature of the substrate has a significant influence on the catalyst surface properties. It shows that, in surface-modified catalysts, the interactions between underlayer and overlayer materials are worthy of consideration, since they can significantly modify the intrinsic properties of the active sites. The measured desorption rates are also lower than those obtained for the commercial PtRu/C catalyst. With regard to the issue of CO tolerance, the kinetics of the CO desorption and CO electrooxidation processes cannot be directly compared for the investigated system due to unavailability of CO oxidation rate values. The measured CO desorption rates are however likely to be large compared to the expected CO oxidation rates: the CO desorption process may thus play a significant role in the CO tolerance issue at such a PEM fuel cell anode and the “detoxification” mechanism may be the

major mechanism to explain the CO tolerance. It has however to be pointed out that these conclusions are “first approach” conclusions due to the unavailability of CO oxidation data for the investigated system, and thus that CO oxidation data for this Pt-on-Au/C system need to be measured, if we are to validate these “first approach” conclusions. The desorption rate constants determined in this study have been also measured in a simplified environment (no humidification, no potential field) and both humidification and potential field may play a role in the balance between desorption and CO oxidation via the bifunctional mechanism within the operating fuel cell environment. This work on the temperature-dependent kinetics of the CO desorption process on a novel Pt-on-Au/C PEMFC anode catalyst supplements the literature data obtained previously for the more traditional Pt and PtRu catalysts. The determination of the CO desorption rate constants on novel PEMFC anode catalysts is believed to be of added value for a better understanding of the CO tolerance issue at PEMFC anodes and if we are to develop novel low cost and CO tolerant catalysts based on the fundamental understanding of the processes involved.

Acknowledgments

This work was carried out within the multi-annual programme of the European Commission's Joint Research Centre and with relation to the Framework Programme 6 (FP6) Specific Targeted Research Project (STREP) “FCAnode” (Non-noble Catalysts for Proton Exchange Membrane Fuel Cell Anodes). The authors would like to thank Miguel Prieto for TEM sample preparation, Jacob van Eijk for the XRD measurements and Marc Steen for critical reading of the manuscript. CINF is supported by the Danish National Research Foundation.

References

- [1] S. Gottesfeld, T.A. Zawodzinski, Polymer electrolyte fuel cells Advances in Electrochemical Science and Engineering, Vol.5, Wiley-VCH, 1997, pp. 195–301.
- [2] W. Vogel, J. Lundquist, P. Ross, P. Stonehart, Reaction pathways and poisons. II. The rate controlling step for electrochemical oxidation of hydrogen on Pt in acid and poisoning of the reaction by CO, *Electrochim. Acta* 20 (1975) 79–93.
- [3] J.J. Baschuk, X. Li, Carbon monoxide poisoning of proton exchange membrane fuel cells, *Int. J. Energy Res.* 25 (2001) 695–713.
- [4] T.R. Ralph, M.P. Hogarth, Catalysis for low temperature fuel cells, *Platinum Met. Rev.* 46 (2002) 117–135.
- [5] M.P. Hogarth, T.R. Ralph, Catalysis for low temperature fuel cells, *Platinum Met. Rev.* 46 (2002) 146–164.
- [6] H.A. Gasteiger, N. Markovic, P.N. Ross, H₂ and CO electrooxidation on well-characterized Pt, Ru, and Pt–Ru. 1. Rotating disk electrode studies of the pure gases including temperature effects, *J. Phys. Chem.* 99 (1995) 8290–8301.
- [7] H.A. Gasteiger, N. Markovic, P.N. Ross, H₂ and CO electrooxidation on well-characterized Pt, Ru, and Pt–Ru. 2. Rotating disk electrode studies of CO/H₂ mixtures at 62 °C, *J. Phys. Chem.* 99 (1995) 16757–16767.
- [8] J.C. Davies, B.E. Hayden, D.J. Pegg, The electrooxidation of carbon monoxide on ruthenium modified Pt(110), *Electrochim. Acta* 44 (1998) 1181–1190.
- [9] J.C. Davies, B.E. Hayden, D.J. Pegg, The modification of Pt(110) by ruthenium: CO adsorption and electro-oxidation, *Surf. Sci.* 467 (2000) 118–130.
- [10] J.C. Davies, B.E. Hayden, M.E. Rendall, D.J. Pegg, The electro-oxidation of carbon monoxide on ruthenium modified Pt(111), *Surf. Sci.* 496 (2002) 110–120.
- [11] S. Desai, M. Neurock, A first principles analysis of CO oxidation over Pt and Pt_{66.7%}Ru_{33.3%} (111) surfaces, *Electrochim. Acta* 48 (2003) 3759–3773.
- [12] M.T.M. Koper, T.E. Shubina, R.A. van Santen, Periodic density functional study of CO and OH adsorption on Pt–Ru alloy surfaces: implications for CO tolerant fuel cell catalysts, *J. Phys. Chem. B* 106 (2002) 686–692.
- [13] Q. Ge, S. Desai, M. Neurock, K. Kourtakis, CO adsorption on Pt–Ru surface alloys and on the surface of Pt–Ru bulk alloy, *J. Phys. Chem. B* 105 (2001) 9533–9536.
- [14] Y. Ishikawa, M.-S. Liao, C.R. Cabrera, Energetics of H₂O dissociation and CO_{ads} + OH_{ads} reaction on a series of Pt–M mixed metal clusters: a relativistic density-functional study, *Surf. Sci.* 513 (2002) 98–110.
- [15] E. Christoffersen, P. Liu, A. Ruban, H.L. Skriver, J.K. Nørskov, Anode materials for low-temperature fuel cells: a density functional theory study, *J. Catal.* 199 (2001) 123–131.
- [16] H. Igarashi, T. Fujino, Y.M. Zhu, H. Uchida, M. Watanabe, CO tolerance of Pt alloy electrocatalysts for polymer electrolyte fuel cells and the detoxification mechanism, *Phys. Chem. Chem. Phys.* 3 (2001) 306–314.
- [17] J.C. Davies, G. Tsotridis, Temperature-dependent kinetic study of CO desorption from Pt PEM fuel cell anodes, *J. Phys. Chem. C* 112 (2008) 3392–3397.

- [18] A. Pitois, J.C. Davies, A. Pilega, A. Pfrang, G. Tsotridis, Kinetic study of CO desorption from PtRu/C PEM fuel cell anodes: temperature dependence and associated microstructural transformations, *J. Catal.* 265 (2009) 199–208.
- [19] F. Buatier de Mongeot, M. Scherer, B. Gleich, E. Kopatzki, R.J. Behm, CO adsorption and oxidation on bimetallic Pt/Ru(0001) surfaces—a combined STM and TPD/TPR study, *Surf. Sci.* 411 (1998) 249–262.
- [20] J.C. Davies, J. Bonde, A. Logadottir, J.K. Nørskov, I. Chorkendorff, The ligand effect: CO desorption from Pt/Ru catalysts, *Fuel Cells* 5 (2005) 429–435.
- [21] H.A. Gasteiger, N. Markovic, P.N. Ross, E.J. Cairns, Carbon monoxide electrooxidation on well-characterized platinum–ruthenium alloys, *J. Phys. Chem.* 98 (1994) 617–625.
- [22] H.F. Oetjen, V.M. Schmidt, U. Stimming, F. Trila, Performance data of a proton exchange membrane fuel cell using H₂/CO as fuel gas, *J. Electrochem. Soc.* 143 (1996) 3838–3842.
- [23] J. Greeley, T.F. Jaramillo, J. Bonde, I. Chorkendorff, J.K. Nørskov, Computational high-throughput screening of electrocatalytic materials for hydrogen evolution, *Nature Mater.* 5 (2006) 909–913.
- [24] J. Greeley, J.K. Nørskov, Large-scale, density functional theory-based screening of alloys for hydrogen evolution, *Surf. Sci.* 601 (2007) 1590–1598.
- [25] J.W.A. Sachtler, G.A. Somorjai, Influence of ensemble size on CO chemisorption and catalytic *n*-hexane conversion by Au–Pt(111) bimetallic single-crystal surfaces, *J. Catal.* 81 (1983) 77–94.
- [26] H. Moller, P.C. Pistorius, The electrochemistry of gold–platinum alloys, *J. Electroanal. Chem.* 570 (2004) 243–255.
- [27] D. Zhao, B.-Q. Xu, Platinum covering of gold nanoparticles for utilization enhancement of Pt in electrocatalysts, *Phys. Chem. Chem. Phys.* 8 (2006) 5106–5114.
- [28] P. Hernandez-Fernandez, S. Rojas, P. Ocon, A. de Frutos, J.M. Figueroa, P. Pereros, M.A. Pena, J.L.G. Fierro, Relevance of the nature of bimetallic PtAu nanoparticles as electrocatalysts for the oxygen reduction reaction in the presence of methanol, *J. Power Sources* 177 (2008) 9–16.
- [29] L. Yang, J. Chen, X. Zhong, K. Cui, Y. Xu, Y. Kuang, Au@Pt nanoparticles prepared by one-phase protocol and their electrocatalytic properties for methanol oxidation, *Colloids Surf. A* 295 (2007) 21–26.
- [30] I.-S. Park, K.-S. Lee, Y.-H. Cho, H.-Y. Park, Y.-E. Sung, Methanol electro-oxidation on carbon-supported and Pt-modified Au nanoparticles, *Catal. Today* 132 (2008) 127–131.
- [31] I.-S. Park, K.-S. Lee, D.-S. Jung, H.-Y. Park, Y.-E. Sung, Electrocatalytic activity of carbon-supported Pt–Au nanoparticles for methanol electro-oxidation, *Electrochim. Acta* 52 (2007) 5599–5605.
- [32] J.-H. Choi, K.-W. Park, I.-S. Park, K. Kim, J.-S. Lee, Y.-E. Sung, A PtAu nanoparticle electrocatalyst for methanol electro-oxidation in direct methanol fuel cells, *J. Electrochem. Soc.* 153 (2006) A1812–A1817.
- [33] I.-S. Park, K.-S. Lee, J.-H. Choi, H.-Y. Park, Y.-E. Sung, Surface structure of Pt-modified Au nanoparticles and electrocatalytic activity in formic acid electro-oxidation, *J. Phys. Chem. C* 111 (2007) 19126–19133.
- [34] J.B. Xu, T.S. Zhao, Z.X. Liang, Carbon supported platinum–gold alloy catalyst for direct formic acid fuel cells, *J. Power Sources* 185 (2008) 857–861.
- [35] D. Zhao, B.-Q. Xu, Enhancement of Pt utilization in electrocatalysts by using gold nanoparticles, *Angewand. Chem. Int. Ed.* 45 (2006) 4955–4959.
- [36] K.A. Friedrich, F. Henglein, U. Stimming, W. Unkauf, Investigation of Pt particles on gold substrates by IR spectroscopy: particle structure and catalytic activity, *Colloids Surf. A* 134 (1998) 193–206.
- [37] K.A. Friedrich, F. Henglein, U. Stimming, W. Unkauf, Size dependence of the CO monolayer oxidation on nanosized Pt particles supported on gold, *Electrochim. Acta* 45 (2000) 3283–3293.
- [38] M.O. Pedersen, S. Helveg, A. Ruban, I. Stensgaard, E. Laegsgaard, J.K. Nørskov, F. Besenbacher, How a gold substrate can increase the reactivity of a Pt overlayer, *Surf. Sci.* 426 (1999) 395–409.
- [39] F. Gao, Y. Wang, D.W. Goodman, CO oxidation over AuPd(100) from ultrahigh vacuum to near-atmospheric pressures: CO adsorption-induced surface segregation and reaction kinetics, *J. Phys. Chem. C* 113 (2009) 14993–15000.
- [40] F. Gao, Y. Wang, D.W. Goodman, CO oxidation over AuPd(100) from ultrahigh vacuum to near-atmospheric pressures: the critical role of contiguous Pd atoms, *J. Am. Chem. Soc.* 131 (2009) 5734–5735.
- [41] B. Gleich, M. Ruff, R.J. Behm, Correlation between local substrate structure and local chemical properties: CO adsorption on well-defined bimetallic Au/Pd(111) surfaces, *Surf. Sci.* 386 (1997) 48–55.
- [42] F. Maroun, F. Ozanam, O.M. Magnussen, R.J. Behm, The role of atomic ensembles in the reactivity of bimetallic electrocatalysts, *Science* 293 (2001) 1811–1814.
- [43] A. Pitois, A. Pilega, G. Tsotridis, CO desorption kinetics at concentrations and temperatures relevant to PEM fuel cells operating with reformat gas and PtRu/C anodes, *Appl. Catal. A* 374 (2010) 95–102.
- [44] J.C. Davies, R.M. Nielsen, L.B. Thomsen, I. Chorkendorff, A. Logadottir, Z. Lodziana, J.K. Nørskov, W.X. Li, B. Hammer, S.R. Longwitz, J. Schnadt, E.K. Vestergaard, R.T. Vang, F. Besenbacher, CO desorption rate dependence on CO partial pressure over platinum fuel cell catalysts, *Fuel Cells* 4 (2004) 309–319.
- [45] M. Heinen, Y.-X. Chen, Z. Jusys, R.J. Behm, Room temperature CO adsorption/exchange kinetics on Pt electrodes—a combined in situ IR and mass spectrometry study, *ChemPhysChem* 8 (2007) 2484–2489.
- [46] J. van Muylder, N. de Zoubov, M. Pourbaix, in: M. Pourbaix (Ed.), *Atlas of Electrochemical Equilibria in Aqueous Solutions*, Pergamon Press, Oxford, 1966, p. 378.
- [47] B.L. Abrams, P.C.K. Vesborg, J.L. Bonde, T.F. Jaramillo, I. Chorkendorff, Dynamics of surface exchange reactions between Au and Pt for HER and HOR, *J. Electrochem. Soc.* 156 (2009) B273–B282.
- [48] M. Xu, E. Iglesia, Readsorption and adsorption-assisted desorption of CO₂ on basic solids, *J. Phys. Chem. B* 102 (1998) 961–966.
- [49] A. Ruban, B. Hammer, P. Stoltze, H.L. Skriver, J.K. Nørskov, Surface electronic structure and reactivity of transition and noble metals, *J. Mol. Catal. A* 115 (1997) 421–429.
- [50] B. Zhang, J.-F. Li, Q.-L. Zhong, B. Ren, Z.-Q. Tian, S.-Z. Zou, Electrochemical and surface-enhanced raman spectroscopic investigation of CO and SCN-adsorbed on Aucore-Ptshell nanoparticles supported on GC electrodes, *Langmuir* 21 (2005) 7449–7455.
- [51] S. Kumar, S. Zou, Electrooxidation of carbon monoxide and methanol on platinum-overlayer-coated gold nanoparticles: effects of film thickness, *Langmuir* 23 (2007) 7365–7371.
- [52] J. Zeng, J. Yang, J.Y. Lee, W. Zou, Preparation of carbon-supported core-shell Au–Pt nanoparticles for methanol oxidation reaction: the promotional effect of the Au core, *J. Phys. Chem. B* 110 (2006) 24606–24611.
- [53] P. Liu, J.K. Nørskov, Ligand and ensemble effects in adsorption on alloy surfaces, *Phys. Chem. Chem. Phys.* 3 (2001) 3814–3818.